Magneto-exciton-polariton condensation in a sub-wavelength high contrast grating based vertical microcavity

J. Fischer, S. Brodbeck, B. Zhang, Z. Wang, L. Worschech, H. Deng, M. Kamp, C. Schneider, and S. Höfling

Citation: Applied Physics Letters **104**, 091117 (2014); doi: 10.1063/1.4866776
View online: http://dx.doi.org/10.1063/1.4866776
View Table of Contents: http://scitation.aip.org/content/aip/journal/apl/104/9?ver=pdfcov
Published by the AIP Publishing

Magneto-exciton-polariton condensation in a sub-wavelength high contrast grating based vertical microcavity

J. Fischer,[1] S. Brodbeck,[1] B. Zhang,[2] Z. Wang,[2] L. Worschech,[1] H. Deng,[2] M. Kamp,[1] C. Schneider,[1] and S. Höfling[1,a)]
[1]*Technische Physik, Physikalisches Institut and Wilhelm Conrad Röntgen-Research Center for Complex Material Systems, Universität Würzburg, Am Hubland, D-97074 Würzburg, Germany*
[2]*Department of Physics, University of Michigan, Ann Arbor, Michigan 48109, USA*

(Received 23 January 2014; accepted 9 February 2014; published online 4 March 2014)

We comparably investigate the diamagnetic shift of an uncoupled quantum well exciton with a microcavity exciton-polariton condensate on the same device. The sample is composed of multiple GaAs quantum wells in an AlAs microcavity, surrounded by a Bragg reflector and a sub-wavelength high contrast grating reflector. Our study introduces an independent and easily applicable technique, namely, the measurement of the condensate diamagnetic shift, which directly probes matter contributions in polariton condensates and hence discriminates it from a conventional photon laser. © *2014 AIP Publishing LLC*. [http://dx.doi.org/10.1063/1.4866776]

Exciton-polaritons arise from the strong coupling[1] between quantum well (QW) excitons and photons in microcavity resonators. Due to their small effective mass and their capability to efficiently cool to common energy states via stimulated scattering, they are ideal candidates to observe dynamic Bose-Einstein-condensation (BEC) in solid-state systems at elevated temperatures.[2–7] In a strictly two-dimensional system, it is not expected to observe a BEC, hence additional trapping techniques are required to facilitate the condensation process. Lately, many approaches of tailoring the dimensionality and trapping the polaritons have been reported, such as etching micropillar cavities,[8,9] strain,[3] metallic layer deposition on the surface,[10] and modulation of the cavity length.[11,12] Since a polariton condensate shares many similarities with a microcavity photon laser, it is important to establish criteria how to unambiguously distinguish the two phenomena. In particular in a low dimensional microcavity condensate, where the effective mass of the polaritons cannot be assessed with high accuracy due to finite size effects, other tools have to be identified. Recently, we have suggested to utilize the interaction with external magnetic fields to quantify the matter content of a polariton laser mode via the magnetic field splitting, both in optically as well as electrically driven polariton lasers.[13,14] Unfortunately, this method cannot be applied to all polariton lasers, in particular to polariton lasers with either a linewidth which is too broad to resolve the Zeeman splitting for accessible magnetic fields or if a strong linear polarization is imposed by the mirror geometry.[16,17] In the latter case, the strong light-matter coupling will be present only for the linearly polarized mode and a formed condensate cannot support the left and right hand circularly polarized modes characterizing the Zeeman splitting.

In this Letter, we focus on the latter case and provide an alternative method which utilizes the magnetic field for directly probing and quantifying matter contributions of polariton condensates.

The sample is composed of 12 GaAs quantum wells integrated in a $\frac{\lambda}{2}$-thick AlAs microcavity. The bottom distributed Bragg reflector (DBR) is a conventional AlAs/AlGaAs DBR, whereas we replaced most parts of the top DBR by a high contrast sub-wavelength grating (SWG).[15] A cross-sectional scanning electron microscope (SEM) image of the epitaxial structure is shown in Fig. 1(a). The finite size of the lithographically defined SWG ($5 \times 5\,\mu$m) provides the required trapping potential to facilitate polariton condensation. As our grating is composed of a configuration of one dimensional wires (see Fig. 1(b)), only the polarization component along the grating wires (which we will refer to as TE polarization in the following) can strongly couple with the excitons, whereas the perpendicular polarization does not strongly couple with the excitons. Additionally, the area surrounding the SWG remains unstructured, which conveniently allows us to comparably probe polaritons versus excitons within the same sample area without additional processing steps (such as removing part of the mirrors via etching). For further details on the sample fabrication or design, we refer the reader to Zhang *et al.*[16]

First, we investigate the power dependent emission features to collect initial indications of polariton condensation in our selected SWG microcavity: The sample is excited non-resonantly at normal incidence with a pulsed

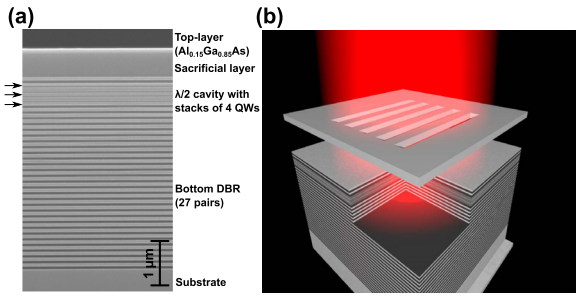

FIG. 1. (a) SEM image of the epitaxial structure which is utilized for the device fabrication. It consists of a $\frac{\lambda}{2}$−cavity with three stacks of 4 QWs. The position of the QWs is indicated by arrows. (b) Schematic sketch of the structure after etching and fabrication steps.

a)Present address: SUPA, School of Physics and Astronomy, University of St. Andrews, St. Andrews, KY16 9SS, United Kingdom

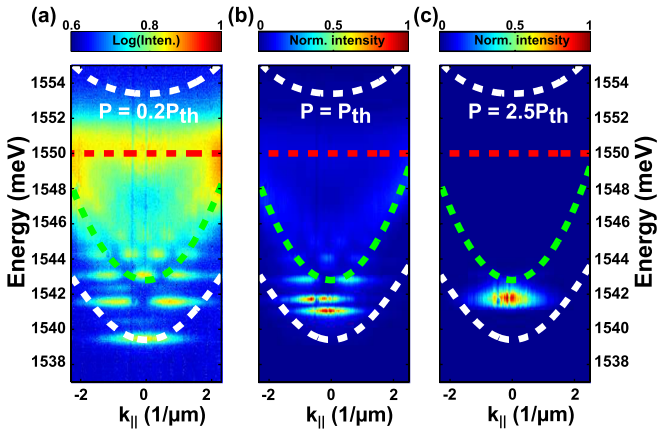

FIG. 2. (a)–(c) Energy-momentum dispersions of a 5 μm large high index contrast grating structure at a detuning of $\delta = -7$ meV. The white dashed lines are indicating the lower and upper polaritons, the red dashed line the exciton, and the green dashed one the photon energy. (a) Well below the non-linearity threshold at $P = 0.2P_{th}$, the zero-dimensional resonances are clearly visible confirming the 3D confinement of the structure. (b) At the threshold $P = P_{th}$, the ground state energy is slightly blueshifted and becomes more and more intensive. Above threshold (c) at $P = 2.5P_{th}$ only the ground state is observable. The emission occurs well below the photon energy (green dashed line) indicating that strong coupling is preserved.

Ti-Sapphire laser (spot size $\sim$4 μm). The excitation wavelength of the laser is set to be about $\sim$80 meV above the lower polariton energy, and the pulse width of the laser is about $\sim$4 ps with a repetition rate of 82 MHz. The sample is held at $T = 6$ K in a helium flow cryostat and a magnetic field up to $B = 5$ T can be applied in Faraday-configuration along the growth axis of the structure. The selected device comprises a detuning between microcavity photon energy E_C and QW exciton energy E_X of $\delta = E_C - E_X = -7$ meV (see Fig. 2(a)), the Rabi-splitting is determined to $E_{RS} = 12$ meV, and an exciton-energy of $E_X = 1.550$ eV was extracted.

Figs. 2(a)–2(c) depict the recorded far-field energy-momentum dispersion spectra of the device at three different excitation power densities.

As a result of the finite structure size, discrete modes dominate the emission spectrum of the cavity. The spectrum for low excitation power $P = 0.2P_{th}$ is plotted in Fig. 2(a). By increasing the excitation power, the emission from the ground state is blue shifted and becomes more intense with respect to the higher discrete modes (Fig. 2(b)). With further increasing the pump power ($P = 2.5P_{th}$ in Fig. 2(c)) the emission blueshifts towards the uncoupled photon resonance at $E_C = 1.543$ eV.

In order to obtain a quantitative picture of these properties, we evaluate the emission properties of the ground state (integrated over a momentum range of $k_{||} = \pm 0.15\ \frac{1}{\mu m}$) as a function of the excitation power. The corresponding input-output characteristic is shown in Fig. 3(a). We can observe a clear threshold behavior at a power of $P_{th} = 575\ \mu$W, which is accompanied by a drop in the emission linewidth (Fig. 3(b)) as a signature of increased temporal coherence.[2,3] The subsequent linewidth broadening and the persisting blueshift of the emission energy are commonly attributed to polariton-polariton repulsive interaction in a massively occupied energy state leading to a renormalization of the chemical potential. In general, these power dependent emission properties are characteristic for polariton condensation under non-resonant pumping,[2,3,9,18] which can, however, be mimicked to some extent by microcavity photon lasers.[19]

In order to directly verify the persistence of the strong coupling above the lasing threshold, we study the interaction of the laser mode with the magnetic field (applied in Faraday configuration). In Fig. 4(a), we plot spectra extracted from $k_{||} = 0$ for magnetic fields between $B = 0$ T and $B = 5$ T, recorded above the nonlinearity threshold at $P = 1.4P_{th}$. The asymmetric shape of the emission peak is due to the pulsed excitation scheme[20] as a result of the time integrated measurement. With increasing magnetic field, the peak energy of the system successively shifts towards higher energies. As we will show in the following, this shift can directly be connected to the diamagnetic shift of the QW exciton emission band, which is given by

$$\Delta E_X = \kappa_X B^2 . \tag{1}$$

Here, κ_X is the diamagnetic coefficient of the QW exciton. For comparison, the diamagnetic shift of the bare QW exciton, recorded under low excitation powers is shown in Fig. 4(b). As expected, the QW exciton emission is also subject to a blueshift in the presence of a magnetic field, however, with a significantly larger magnitude. In contrast to a standard microcavity composed of two DBR segments, we can directly probe the uncoupled QW luminescence simply by moving the collection spot a few μm away from the SWG, hence allowing for a high degree of comparability. In Fig. 4(c), we plot the peak position of both the emission features from the coupled and the uncoupled system as a function of the magnetic field. The diamagnetic coefficient of the QW exciton which amounts to $\kappa_{X,low\,P} = 57\ \mu$eV/T^2 is

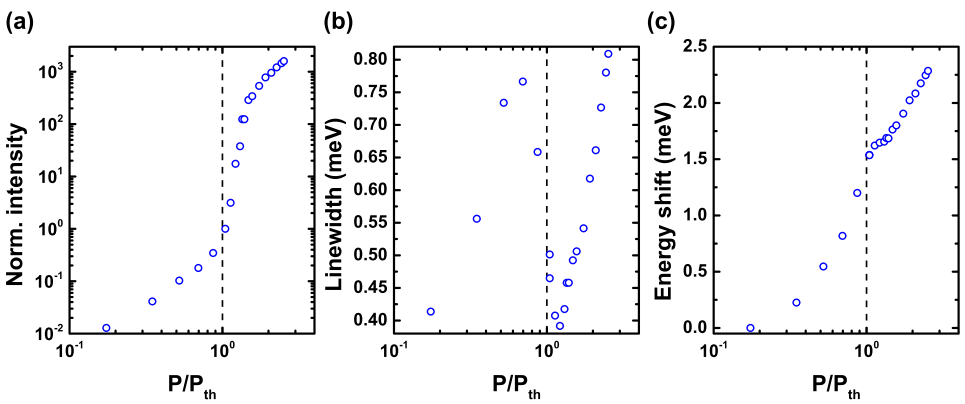

FIG. 3. (a) Input-output curve and (b) power dependent linewidth trace of the ground state emission. Slightly above threshold, the linewidth narrows down to 0.391 meV (smaller than for low excitation powers). (c) Energy peak position versus excitation power. All the values are extracted from the momentum-space spectra by integrating around $k_{||} = 0$ with $k_{||} = \pm 0.15\ \frac{1}{\mu m}$.

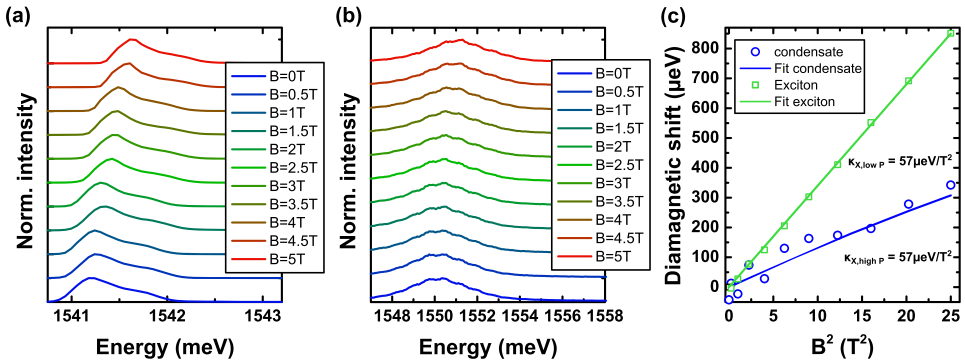

FIG. 4. Line spectra from the momentum-space images for the different magnetic fields from $B = 0$ T to $B = 5$ T at an excitation power of $P = 1.4P_{th}$ for (a) the polariton condensate and (b) the uncoupled QW exciton. (c) Comparison between the diamagnetic shift of the bare quantum well exciton (green squares) and the diamagnetic shift of the polariton condensate (blue dots).

determined straight forwardly by fitting the data with Eq. (1). In order to theoretically reproduce the diamagnetic shift of the polariton condensate, we have to extend the simple expression Eq. (1) by including the effects of light-matter hybridization via a polariton Hopfield coefficient $|X(\kappa_X, B, E_{RS})|^2$. The latter characterizes the degree of light-matter hybridization in the system

$$\Delta E_{Dia,LP} = |X(\kappa_X, B, E_{RS})|^2 \kappa_X B^2. \quad (2)$$

For the detuning of our device $\delta = -7$ meV and the Rabi-splitting of $E_{RS} = 12$ meV, the matter part in our device amounts to $|X|^2 = 0.24$ at 0 T.

When a magnetic field is applied, the exciton-photon detuning changes, and the Rabi-splitting increases as a result of an increased exciton oscillator strength.[21] Consequently, the Hopfield coefficient becomes a function of the magnetic field and reads

$$|X(\kappa_X, B, E_{RS})|^2 = \frac{1}{2}\left(1 + \frac{E_C - (E_X + \kappa_X B^2)}{\sqrt{(E_C - (E_X + \kappa_X B^2))^2 + (E_{RS}(B))^2}}\right). \quad (3)$$

By assuming approximately a linear increase of the Rabi-splitting from $E_{RS} = 12$ meV to $E_{RS} = 12.5$ meV between 0 T and 5T,[18] we can fit the data of the polariton condensate's diamagnetic shift in Fig. 4(c) by combining Eqs. (2) and (3).

This allows us to determine the diamagnetic coefficient κ_X of the QW exciton from the polariton condensate's diamagnetic shift at $P = 1.4P_{th}$ (see Fig. 4(c), red solid line) to $\kappa_{X,high\,P} = 57$ μeV/T^2 which is in perfect agreement with the bare exciton shift at low excitation power. This confirms that the model Eq. (2) and the assumptions for the change of the detuning and the Rabi-splitting with magnetic field are well justified. More importantly, it directly evidences the matter contribution in our laser system and justifies the attribution to a polariton condensate. Indeed, for a polariton laser system close to the Mott transition, an increase of the diamagnetic coefficient with increasing exciton densities could be expected as a result of excitonic screening effects.[12] Since our analysis confirms that such an effect can be neglected in our experiment, we conclude that our low dimensional SWG laser is not only operated in the strong light-matter coupling regime but also significantly below the transition to the weak coupling crossover.

In conclusion, we have demonstrated polariton condensation in a hybrid microcavity structure with multiple QWs, where the top DBR is replaced by a sub wavelength high contrast grating. We observe all typical power dependent emission properties for a polariton condensate. Additionally, we demonstrate that the diamagnetic shift of the condensate emission is a powerful tool to probe the hybrid light-matter character of such a coupled system by directly and quantitatively relating the condensate's shift to the exciton diamagnetic shift.

Technical assistance by M. Wagenbrenner during sample fabrication, as well as M. Amthor and S. Holzinger during the measurements is gratefully acknowledged. This work has been supported by the State of Bavaria, the National Science Foundation of the United States (OISE 1132725), and the U.S. Air Force Office of Scientific Research (FA9550-12.1.0256).

[1]C. Weisbuch, M. Nishioka, A. Ishikawa, and Y. Arakawa, Phys. Rev. Lett. **69**, 3314–3317 (1992).
[2]J. Kasprzak, M. Richard, S. Kundermann, A. Baas, P. Jeambrun, J. M. J. Keeling, F. M. Marchetti, M. H. Szymańska, R. André, J. L. Staehli, V. Savona, P. B. Littlewood, B. Deveaud, and L. S. Dang, Nature **443**, 409–414 (2006).
[3]R. Balili, V. Hartwell, D. Snoke, L. Pfeiffer, and K. West, Science **316**, 1007–1010 (2007).
[4]H. Deng, G. Weihs, C. Santori, J. Bloch, and Y. Yamamoto, Science **298**, 199–202 (2002).
[5]S. Christopoulos, G. B. H. von Högersthal, A. J. D. Grundy, P. G. Lagoudakis, A. V. Kavokin, J. J. Baumberg, G. Christmann, R. Butté, E. Feltin, J.-F. Carlin, and N. Grandjean, Phys. Rev. Lett. **98**, 126405 (2007).
[6]H. Deng, H. Haug, and Y. Yamamoto, Rev. Mod. Phys. **82**, 1489 (2010).
[7]J. D. Plumhof, T. Stöferle, L. Mai, U. Scherf, and R. F. Mahrt, Nat. Mat. **13**, 247 (2014).
[8]T. Gutbrod, M. Bayer, A. Forchel, J. P. Reithmaier, T. L. Reinecke, S. Rudin, and P. A. Knipp, Phys. Rev. B **57**, 9950 (1998).
[9]D. Bajoni, P. Senellart, E. Wertz, I. Sagnes, A. Miard, A. Lemaître, and J. Bloch, Phys. Rev. Lett **100**, 047401 (2008).
[10]S. Utsunomiya, L. Tian, G. Roumpos, C. W. Lai, N. Kumada, T. Fujisawa, M. Kuwata-Gonokami, A. Löffler, S. Höfling, A. Forchel, and Y. Yamamoto, Nat. Phys. **4**, 700 (2008).
[11]O. El Daïf, A. Baas, T. Guillet, J.-P. Brantut, R. I. Kaitouni, J. L. Staehli, F. Morier-Genoud, and B. Deveaud, Appl. Phys. Lett. **88**, 061105 (2006).
[12]A. Rahimi-Iman, C. Schneider, J. Fischer, S. Holzinger, M. Amthor, S. Höfling, S. Reitzenstein, L. Worschech, M. Kamp, and A. Forchel, Phys. Rev. B **84**, 165325 (2011).
[13]J. Fischer, S. Brodbeck, A. Chernenko, I. Lederer, A. Rahimi-Iman, M. Amthor, V. D. Kulakovskii, L. Worschech, M. Kamp, M. Durnev, C. Schneider, A. V. Kavokin, and S. Höfling, "Anomalies of a Nonequilibrium Spinor Polariton Condensate in a Magnetic Field," Phys. Rev. Lett. (to be published).
[14]C. Schneider, A. Rahimi-Iman, N. Y. Kim, J. Fischer, I. G. Savenko, M. Amthor, M. Lermer, A. Wolf, L. Worschech, V. D. Kulakovskii,

I. A. Shelykh, M. Kamp, S. Reitzenstein, A. Forchel, Y. Yamamoto, and S. Höfling, Nature **497**, 348–352 (2013).
[15]M. Huang, Y. Zhou, and C. Chang-Hasnain, Nat. Photonics **1**, 119 (2007).
[16]B. Zhang, Z. Wang, S. Brodbeck, C. Schneider, M. Kamp, S. Höfling, and H. Deng, Light: Sci. Appl. **3**, e135 (2014).
[17]S. Azzini, D. Gerace, M. Galli, I. Sagnes, R. Braive, A. Lemaître, J. Bloch, and D. Bajoni, Appl. Phys. Lett. **99**, 111106 (2011).
[18]G. Roumpos, W. H. Nitsche, S. Höfling, A. Forchel, and Y. Yamamoto, Phys. Rev. Lett. **104**, 126403 (2010).
[19]D. Bajoni, P. Senellart, A. Lemaître, and J. Bloch, Phys. Rev. B **76**, 201305(R) (2007).
[20]E. Kammann, H. Ohadi, M. Maragkou, A. V. Kavokin, and P. G. Lagoudakis, New J. Phys. **14**, 105003 (2012).
[21]T. A. Fisher, A. M. Afshar, M. S. Skolnick, D. M. Whittaker, and J. S. Roberts, Phys. Rev. B **53**, R10469 (1996).